International Research Journal of Earth Sciences ISSN 2321–2527
Vol. **3(7),** 1-10, July **(2015)** *Int. Res. J. Earth Sci.*

Examining the Role of Topographic-Bedding Surface Intersection on HILL SLOPE Instability in Mousi River Basin, Garhwal District, Uttarakhand, India

Mukunda Mishra
Dept. of Geography, Dr. Meghnad Saha College, Itahar, Uttar Dinajpur, W.B. 733128, INDIA

Available online at: www.isca.in, www.isca.me
Received 29th June 2015, revised 3rd July 2015, accepted 22nd July 2015

Abstract

The question of stability of slopes exhibits its frequent presence in most part of the Garhwal Himalayas in the form of creeping, rock falls and slides of varying magnitudes leading to a degree of damages to human lives and resources. It is well known that the process of hill slope instability is a multi-causal phenomena and the topographic-geologic surface intersection plays a vital role in it. The effort has been made in the present study to examine this specific factor in a particular river basin unit through field data collection and statistical analysis on it for reaching towards a rational conclusion.

Keywords: Cataclinal, anaclinal, orthoclinal, landslide, hill slope instability.

Introduction

The phenomenon of hill slope instability is a typical process resulted from the complicated interaction of different geologic, tectonic and geomorphic factors along with a vital role of anthropogenic activities over the slopes; and this process results into a certain degree of loss of human lives and resources at different part of the world which has added another perspective of studying the process from the standpoint of 'environmental hazard'. As Smith mentioned that the term 'environmental hazard' has the advantage of including both natural and human dimensions; besides, this dual perspective also bring forth enormous scholarly debate to establish whether a particular hazard has greater influence from nature or man[1].

However, there is a generalized understanding – if the degree of responsibility of individual human being is concerned, the responsibility factor increases greatly from the large scale geophysical hazards (e.g. earthquake) towards the social hazards (e.g. smoking) that are largely self-induced in nature. When the issue of slope instability is concerned, the geological and structural settings of slopes are considered as the main predisposing factors for the scientific observations and analysis of the phenomena of hill slope instability[2-4]. Bedding of lithological sequences with complexity of arrangements[5,6], the issues of contacts – stratigraphic or tectonic, between rocks with varying geo-mechanical and severely fractured zones that are linked to the presence of axes of folds and faults etc are all favorable geological conditions towards making the hill slope instable[7,8]. The observations of these elements at different scales play fundamental role in understanding the slope instability mechanism. When the targeted process for observation and measurement is allied with the landslide, then it is the bedding planes of layered formations that can control both the landslide mechanism and the activity, in terms of style, magnitude and distribution[9]. The analysis of the relationship between bedding plain attitude and topography may be considered as one of the key procedures to identify and comprehend how far a particular slope unit is controlled by structural parameters. This is also to be noted that the geometric relationships between topography and geologic structure influences the process of sub-surface drainage and mass wasting of a particular slope unit[10,11]. The present study tries to examine the influence of geologic-topographic surface intersection on hill slope instability processes in a particular river basin unit.

The present study has been conducted in the basin of the river Mousi, a small southbound river. The river basin is situated at the south-eastern direction of the Mussorrie Town of Garhwal District, Uttarakhand, having a north-south stretching elongated shape. The study area is geographically extended between $78^0$05'00"E - $78^0$07'30"E longitude and $30^0$23'35.2"N – $30^0$29'57"N latitude. The basin covers a total of 17.2 km.^{2} of area. The basin area of river Mousi is located in Lesser Himalaya and it has a close association with the Main Boundary Thrust (MBT) which is a tectonic discontinuity, dipping north-northeast, and bringing the Lesser Himalayan rocks in juxtaposition with the rocks of Siwalicks. The northern part of the study area including the Mussoorie town comes within the zone IV of the Seismic Zonation Map of India[12]. Proximity to the major seismic discontinuity is responsible for fragility of the terrain that consists of highly fractured and sheared rock mass of mostly limestone, dolomitic limestone, calcareous sandy shale, micaceous sandy siltstone, grey and black shale, silty shale, quartzite and chert[13]. The area witnesses the incidences of hill slope instability of varying magnitude and forms, accompanied with a varying degree of structural damages.

Figure-1
Location of the study area

The present study tries – i. to observe the litho-structural-topographic control on hill slope forms and processes; ii. to examine the interrelationship between topographic/bedding plane intersection and hill slope instability and iii. to interpret the relationship for obtaining a concluding remark.

Material and Methods

Assessment of Hill Slope Instability: The degree of hill slope instability cannot be measured directly as it ranges from a very slow process like creep to very rapid process like landslide. The close observations on slope units for identifying the signs or evidences of active or past mass movement processes leads to establish a scaling device to measure the degree of hill slope instability; and the slope units of the present study area reflect distinct evidences of three mass movement processes mainly – creep, rock fall and slide. The assessment of the slope instability has been done using an weighted scoring (table-1) namely Weighted Index of Slope Instability ($0 \leq \xi \leq 10$).

Testing the significance of relationship of slope instability with different morpho-structural parameters individually: Pearson's Correlation Coefficient is used to find out the relationship between different morpho-strutural parameters and the WISI (ξ); and the T-test is applied to determine the significance of relationship in between the them.

Classification of Slopes using Chord Length: Slopes are classified into three categories, namely–cataclinal, anaclinal and orthoclinal, on the basis of the interrelationship between the azimuth of topographic slope (A) and the azimuth of bedding dip (α).

Chord Length (L) = $\sqrt{(\cos\alpha - \cos A)^2 + (\sin\alpha - \sin A)^2}$

Using the value of the magnitude of topographic slope (S) and the bedding dip (Θ), the cataclinal and anaclinal slopes can be further sub-classified[14] (table-2).

Calculating the Topographic-Bedding plane Intersection Angle (TOBIA): This Index has been used by Meentemeyer and Moody[14] through the modification of the logic used for modeling the topographic variability to solar radiation by Dozier[15] and Dubayah[16].

TOBIA (τ) = $\{(\cos\Theta \,.\cos S) + (\sin\Theta \,.\sin S)\,.\cos(\alpha - A)\}$

The value of τ can be used successfully as an index to represent the conformity between topographic and bedding surfaces and the value of this index ranges from one to negative one ($-1 \le \tau \le 1$).

Results and Discussion

The Weighted Index of Slope Instability ($0 \le \xi \le 10$) has been calculated for the observations on randomly selected 43 slope units throughout the basin of river Mousi (table-3).

Table-1
Weighting and Scoring pattern for Weighted Index of Slope Instability (ξ)

Mass movement evident	Degree of Slope Instability	Maximum score to be assigned	Intensity	Score to be assigned
Creep	Low	1	No creep	0.00
			Low	0.33
			Moderate	0.66
			High	1.00
Rock Fall	Moderate	2	No rock fall	0.00
			Slight	0.66
			Moderate	1.33
			Rapid	2.00
Old Landslide	High	3	No scar of old landslide	0.00
			<1000 cubic m. mass displaced	1.00
			1000-2000 cubic m. mass displaced	2.00
			>2000 cubic m. mass displaced	3.00
Active Landslide	Very High	4	No scar of active landslide	0.00
			<1000 cubic m. mass displaced	1.33
			1000-2000 cubic m. mass displaced	2.66
			>2000 cubic m. mass displaced	4.00

Table-2
Classification of Slope Units (after Meentemeyer and Moody, 1994)

Chord Length (L)	Slope Type	(Θ – S)	Sub-category
$0 \le L \le 0.7654$	Cataclinal Slope (a_c)	$(\Theta - S) < -5^0$	Overdip Slope ($a_{c/o}$)
		$-5^0 \le (\Theta - S) \le 5^0$	Dip Slope ($a_{c/d}$)
		$(\Theta - S) > 5^0$	Underdip Slope ($a_{c/u}$)
$0.7654 < L \le 1.8478$	Orthoclinal Slope (a_o)	-	-
$1.8478 < L \le 2$	Anaclinal Slope (a_a)	$(\Theta - S) < -5^0$	Steepened Escarpment ($a_{a/t}$)
		$-5^0 \le (\Theta - S) \le 5^0$	Normal Escarpment ($a_{a/n}$)
		$(\Theta - S) > 5^0$	Subdued Escarpment ($a_{a/s}$)

Table-3
Computation of WISI (ξ) for the observed slope units

Site Sl. No.	Altitude	Magnitude of Creep observed	Magnitude of Rock fall observed	Observations on Land Slide Scars						Weighted Index of Slope Instability
				Height	Width	Breadth	Volume of Scar	Old Slide's Magnitude	Active Slide's Magnitude	
	m.	1/2/3/4	1/2/3/4	m.	m.	m.	m^3	1/2/3/4	1/2/3/4	$0 \leq \xi \leq 10$
A01	1955	1	1	0	0	0	0	0	0	0.99999
A02	1968	1	1	0	0	0	0	0	0	0.99999
A03	1932	1	1	15	10	8	1200	2	0	2.99999
A04	1931	1	1	0	0	0	0	0	0	0.99999
A05	1935	2	2	45	20	12	10800	3	0	4.99998
A06	1958	0	2	0	0	0	0	0	0	1.33332
A07	1939	2	1	0	0	0	0	0	0	1.33332
A08	1870	2	1	0	0	0	0	0	0	1.33332
A09	1853	2	2	25	10	7	1750	0	2	4.66664
A10	1844	1	2	15	10	5	750	1	0	2.66665
A11	1850	1	1	0	0	0	0	0	0	0.99999
A12	1842	1	1	35	18	10	6300	3	0	3.99999
A13	1831	1	1	0	0	0	0	0	0	0.99999
B01	1951	1	1	0	0	0	0	0	0	0.99999
B02	1946	2	3	20	8	5	800	1	0	3.66664
B03	1942	0	3	15	12	10	1800	2	0	3.99998
B04	1937	2	3	25	8	3	600	0	1	3.99997
B05	1889	2	1	22	10	6	1320	0	2	3.99998
B06	1862	3	2	30	15	3	1350	2	0	4.33331
B07	1852	0	1	0	0	0	0	0	0	0.66666
B08	1845	2	2	0	0	0	0	0	0	1.99998
B09	1836	0	1	0	0	0	0	0	0	0.66666
B10	1845	1	1	0	0	0	0	0	0	0.99999
B11	1854	2	1	20	10	6	1200	0	2	3.99998
C01	1796	1	3	18	10	6	1080	0	2	4.99997
C02	1637	1	0	0	0	0	0	0	0	0.33333
C03	1621	0	1	0	0	0	0	0	0	0.66666
C04	1598	0	1	35	20	10	7000	0	3	4.66665
C05	1545	0	0	0	0	0	0	0	0	0
C06	1502	0	0	0	0	0	0	0	0	0
C07	1438	1	1	0	0	0	0	0	0	0.99999
C08	1423	1	1	0	0	0	0	0	0	0.99999
C09	1411	0	0	0	0	0	0	0	0	0
C10	1396	3	2	22	18	10	3960	0	3	6.3333
C11	1383	2	2	15	10	6	900	0	1	3.33331
C12	1369	0	0	25	12	8	2400	3	0	3
D01	1316	3	1	15	8	3	360	0	1	2.99998
D02	1302	0	0	0	0	0	0	0	0	0
D03	1286	1	0	0	0	0	0	0	0	0.33333
D04	1268	1	0	0	0	0	0	0	0	0.33333
D05	1225	1	2	22	10	7	1540	0	2	4.33331
D06	1211	1	0	0	0	0	0	0	0	0.33333
D07	1197	0	0	20	8	3	480	0	1	1.33333

For the above mentioned 43 slope units, the Magnitude of True Dip (ϴ) has been calculated using the collected data of Magnitude (ϴ') as well as Azimuth (α') of Apparent Dip; and Azimuth of True Dip (α) with the help of the following relationship between the Apparent and True Dip of bedding strata (table-4).

$\Theta = \arctan(\tan\Theta'/\cos\delta)$; where, $\delta = (\alpha \sim \alpha')$

Table-4
Converting apparent dip to true dip

Site Sl. No.	Bedding Dip (Apparent) Magnitude (ϴ'; 0-90 Deg.)	Bedding Dip (Apparent) Azimuth (α'; 0-360 Deg.)	Bedding Dip (True) Azimuth (α; 0-360 Deg.)	Difference of Azimuth of Apparent and True Dip (δ = α ~ α')	Bedding Dip (True) Magnitude ϴ = arctan(tan ϴ'/cos δ)
A01	20	95	65	30	23
A02	20	95	65	30	23
A03	50	185	135	50	62
A04	55	95	135	-40	62
A05	50	185	135	50	62
A06	20	95	65	30	23
A07	50	80	135	-55	65
A08	60	295	350	-55	72
A09	6	335	335	0	6
A10	6	335	335	0	6
A11	6	335	335	0	6
A12	6	335	335	0	6
A13	14	125	125	0	14
B01	55	120	190	-70	77
B02	55	120	190	-70	77
B03	40	200	240	-40	47
B04	47	250	250	0	47
B05	11	185	185	0	11
B06	33	275	275	0	33
B07	33	275	275	0	33
B08	25	320	275	45	33
B09	33	275	275	0	33
B10	10	165	120	45	14
B11	10	165	120	45	14
C01	70	235	150	85	88
C02	50	35	70	-35	55
C03	50	35	70	-35	55
C04	20	105	65	40	25
C05	65	315	315	0	65
C06	65	315	315	0	65
C07	70	135	135	0	70
C08	70	135	135	0	70
C09	70	125	135	-10	70
C10	47	240	300	-60	65
C11	50	245	300	-55	65
C12	47	240	300	-60	65
D01	50	95	40	55	65
D02	50	95	40	55	65
D03	15	295	295	0	15
D04	15	295	295	0	15
D05	2	225	225	0	2
D06	2	225	225	0	2
D07	2	225	225	0	2

Now, the values of observed morpho-structural parameters i.e. altitude (h), magnitude of topographic slope (S), azimuth of topographic slope (A), magnitude of bedding dip (Θ) and azimuth of bedding dip (α) are treated as independent variables and WISI (ξ) is treated as dependent variable. Pearson's Correlation Coefficient (r) is calculated for each set (table-5 for detailed dataset of calculation of r). T-test (at 95% confidence level) applied to each set of relationship for testing the null hypothesis that "there is no significant relationship between each individual morpho-structural parameters and WISI (i.e. h with ξ, S with ξ, A with ξ, θ with ξ and α with ξ)".

Table-5
Dataset for Correlation Coefficient (Pearson) computation

Site Sl. No.	Altitude	Topographic Slope		Bedding Dip		WISI
		Magnitude	Azimuth	Magnitude	Azimuth	
	m.	(S)	(A)	(Θ)	(α)	$0 \leq \xi \leq 10$
A01	1955	49	160	23	65	0.99999
A02	1968	43	160	23	65	0.99999
A03	1932	46	120	62	135	2.99999
A04	1931	35	65	62	135	0.99999
A05	1935	56	135	62	135	4.99998
A06	1958	30	220	23	65	1.33332
A07	1939	55	160	65	135	1.33332
A08	1870	51	350	72	350	1.33332
A09	1853	70	280	6	335	4.66664
A10	1844	40	175	6	335	2.66665
A11	1850	51	195	6	335	0.99999
A12	1842	33	290	6	335	3.99999
A13	1831	37	210	14	125	0.99999
B01	1951	41	120	77	190	0.99999
B02	1946	88	95	77	190	3.66664
B03	1942	83	95	47	240	3.99998
B04	1937	89	160	47	250	3.99997
B05	1889	57	185	11	185	3.99998
B06	1862	88	180	33	275	4.33331
B07	1852	35	180	33	275	0.66666
B08	1845	57	80	33	275	1.99998
B09	1836	35	190	33	275	0.66666
B10	1845	45	230	14	120	0.99999
B11	1854	45	100	14	120	3.99998
C01	1796	86	335	88	150	4.99997
C02	1637	13	200	55	70	0.33333
C03	1621	41	190	55	70	0.66666
C04	1598	29	65	25	65	4.66665
C05	1545	4	100	65	315	0
C06	1502	15	95	65	315	0
C07	1438	38	175	70	135	0.99999
C08	1423	45	30	70	135	0.99999
C09	1411	17	280	70	135	0
C10	1396	87	300	65	300	6.3333
C11	1383	64	55	65	300	3.33331
C12	1369	4	275	65	300	3
D01	1316	30	65	65	40	2.99998
D02	1302	27	80	65	40	0
D03	1286	21	70	15	295	0.33333
D04	1268	15	155	15	295	0.33333
D05	1225	77	85	2	225	4.33331
D06	1211	12	60	2	225	0.33333
D07	1197	28	200	2	225	1.33333

Only for the relationship between S and ξ, the $T>T_{0.975(df=x)}$; so, in this case, the null hypothesis is rejected. For rest of the cases, $T<T_{0.975(df=x)}$; hence, Null Hypothesis is accepted; therefore, these relationships are statistically insignificant (table-6).

The test of significance bring to fore the conclusion that altitude, direction of topographic slope and magnitude as well as azimuth of bedding dip, as individual factors, hardly influence the issue of hill slope instability. Only, the magnitude of topographic slope shows significant positive relationship with the degree of slope instability in the area under observation. Under this circumstance a combination of topographic and bedding parameters are required to be correlated with the WISI to interpret the morpho-structural influence on hill slope instability.

The Topographic-Bedding Plane Intersection Angle (TOBIA) has been calculated for each of 43 slope units and also, the slope units are classified into three different classes i.e. Cataclinal (a_c), Anaclinal (a_a) and Orthoclinal (a_o) using the value of Chord Length (L) of the slope units (table-7).

Only for the relationship between S and ξ, the $T>T_{0.975(df=x)}$; so, in this case, the null hypothesis is rejected. For rest of the cases, $T<T_{0.975(df=x)}$; hence, Null Hypothesis is accepted; therefore, these relationships are statistically insignificant. The test of significance bring to fore the conclusion that altitude, direction of topographic slope and magnitude as well as azimuth of bedding dip, as individual factors, hardly influence the issue of hill slope instability. Only, the magnitude of topographic slope shows significant positive relationship with the degree of slope instability in the area under observation. Under this circumstance a combination of topographic and bedding parameters are required to be correlated with the WISI to interpret the morpho-structural influence on hill slope instability.

The Topographic-Bedding Plane Intersection Angle (TOBIA) has been calculated for each of 43 slope units and also, the slope units are classified into three different classes i.e. Cataclinal (a_c), Anaclinal (a_a) and Orthoclinal (a_o) using the value of Chord Length (L) of the slope units.

TOBIA (τ) is placed along X-axis and the Weighted Index of Slope Instability (ξ) is placed along Y-axis for different categories of slopes separately to analyse the association between the two variables.

The scatter diagram of three different kinds of slopes (figure-2) shows very unique response of hill slope instability with the variation of topographic-geologic surface conformity. In each diagrams both the linear and 2nd order polynomial trend lines (continuous and dashed line) are drawn to observe the general trend of relationship as well as the trend of variation of the relationship within the entire range of observations.

To follow Meentemeyer and Moody[14] regarding the response function of TOBIA (τ), as an index for representing the statistical relationship between the conformity between topographic and bedding surfaces, it can be stated that the values of τ for cataclinal slopes range between 0 and 1; for dip-slopes where Θ and S are equivalent, value of τ increases towards ‘1’; whereas value of τ decreases towards ‘0’ when Θ and S become unaligned extremely. In the case of anaclinal slopes, τ decreases if either Θ or S increases away. For the orthoclinal slopes, the cosine value of the difference of azimuth of bedding dip (α) and topographic slope (A) of the TOBIA equation does adjust the value of τ by quantifying the degree to which dip direction and slope aspect are aligned. Here, the τ value ranges from 1 (where, Θ and S are low) to 0 (where, Θ and S are high). From figure 1(a), as the τ become increasing from ‘-1’ to ‘0’ to ‘1’, the value of ξ, representing the instability decreases away. Being the anaclinal slope, the azimuth of surface slope and bedding dip are compass opposite; this implies – when both the Θ and S are low, i.e. τ shows higher value, the ξ index shows lower value; and when the value of Θ and S increase away, the slope becomes comparatively instable envisaged by the higher τ value which results into lowering the ξ value. From figure 1(b), when Θ and S are nearly equivalent to indicate the tendency of the slope to be dip slope and the τ reflects higher value in this circumstance, the value of ξ is also higher. It may be described as the tendency of land slips increases in cataclinal dip slopes. Being the τ value in cataclinal slope ranges between ‘0’ and ‘1’, the value of $\tau > 0.5$ may be casually stated as the situation of geologic surface tending to get equivalent with topographic surface. As the τ value is getting higher, the hill slope is getting instable as shown by comparatively higher value of ξ. From figure 1(c), the value of τ as getting higher, the slope surface is considered to have getting aligned with the bedding; which is accompanied with the lowering tendency of the value of ξ to reflect the observed stability.

Table-6
Testing the significance of relationship

Independent Variable	Dependent Variable	r	N	ν=N-2	r^2	$1-r^2$	T	$T_{.975(df=x)}$
h	ξ	0.194768	43	41	0.037934	0.962066	1.27147	2.0195
S	ξ	0.700565	43	41	0.490791	0.509209	6.286264	2.0195
A	ξ	0.166097	43	41	0.027588	0.972412	1.078518	2.0195
Θ	ξ	-0.01065	43	41	0.000113	0.999887	-0.06818	2.0195
α	ξ	0.136328	43	41	0.018585	0.981415	0.881154	2.0195

Table-7
Classification of slopes and computation of TOBIA (τ)

Site Sl. No.	Topographic Slope		Bedding Dip		Chord Length	Slope Category	Ө-S	Slope Sub Category	TOBIA
	S	A	Ө	α	L				-1≤τ≤+1
A01	49	160	23	65	1.4746	a_o	-26	-	0.578
A02	43	160	23	65	1.4746	a_o	-20	-	0.650
A03	46	120	62	135	0.2611	a_c	16	Underdip Slope	0.940
A04	35	65	62	135	1.1472	a_o	27	-	0.558
A05	56	135	62	135	0.0000	a_c	6	Near-Dip Slope	0.995
A06	30	220	23	65	1.9526	a_a	-7	Near-Normal Escarpment	0.620
A07	55	160	65	135	0.4329	a_c	10	Underdip Slope	0.915
A08	51	350	72	350	0.0000	a_c	21	Underdip Slope	0.934
A09	70	280	6	335	0.9235	a_o	-64	-	0.396
A10	40	175	6	335	1.9696	a_a	-34	Steepened Escarpment	0.699
A11	51	195	6	335	1.8794	a_a	-45	Steepened Escarpment	0.564
A12	33	290	6	335	0.7654	a_c	-27	Overdip Slope	0.874
A13	37	210	14	125	1.3512	a_o	-23	-	0.788
B01	41	120	77	190	1.1472	a_o	36	-	0.388
B02	88	95	77	190	1.4746	a_o	-11	-	-0.077
B03	83	95	47	240	1.9074	a_a	-36	Steepened Escarpment	-0.512
B04	89	160	47	250	1.4142	a_o	-42	-	0.012
B05	57	185	11	185	0.0000	a_c	-46	Overdip Slope	0.695
B06	88	180	33	275	1.4746	a_o	-55	-	-0.018
B07	35	180	33	275	1.4746	a_o	-2	-	0.660
B08	57	80	33	275	1.9829	a_a	-24	Steepened Escarpment	0.016
B09	35	190	33	275	1.3512	a_o	-2	-	0.714
B10	45	230	14	120	1.6383	a_o	-31	-	0.628
B11	45	100	14	120	0.3473	a_c	-31	Overdip Slope	0.847
C01	86	335	88	150	1.9981	a_a	2	Normal Escarpment	-0.991
C02	13	200	55	70	1.8126	a_o	42	-	0.440
C03	41	190	55	70	1.7321	a_o	14	-	0.164
C04	29	65	25	65	0.0000	a_c	-4	Dip Slope	0.998
C05	4	100	65	315	1.9074	a_a	61	Subdued Escarpment	0.370
C06	15	95	65	315	1.8794	a_a	50	Subdued Escarpment	0.229
C07	38	175	70	135	0.6840	a_c	32	Underdip Slope	0.713
C08	45	30	70	135	1.5867	a_o	25	-	0.070
C09	17	280	70	135	1.9074	a_a	53	Subdued Escarpment	0.102
C10	87	300	65	300	0.0000	a_c	-22	Overdip Slope	0.927
C11	64	55	65	300	1.6868	a_o	1	-	-0.159
C12	4	275	65	300	0.4329	a_c	61	Underdip Slope	0.479
D01	30	65	65	40	0.4329	a_c	35	Underdip Slope	0.777
D02	27	80	65	40	0.6840	a_c	38	Underdip Slope	0.692
D03	21	70	15	295	1.8478	a_o	-6	-	0.836
D04	15	155	15	295	1.8794	a_a	0	Normal Escarpment	0.882
D05	77	85	2	225	1.8794	a_a	-75	Steepened Escarpment	0.199
D06	12	60	2	225	1.9829	a_a	-10	Steepened Escarpment	0.971
D07	28	200	2	225	0.4329	a_c	-26	Overdip Slope	0.897

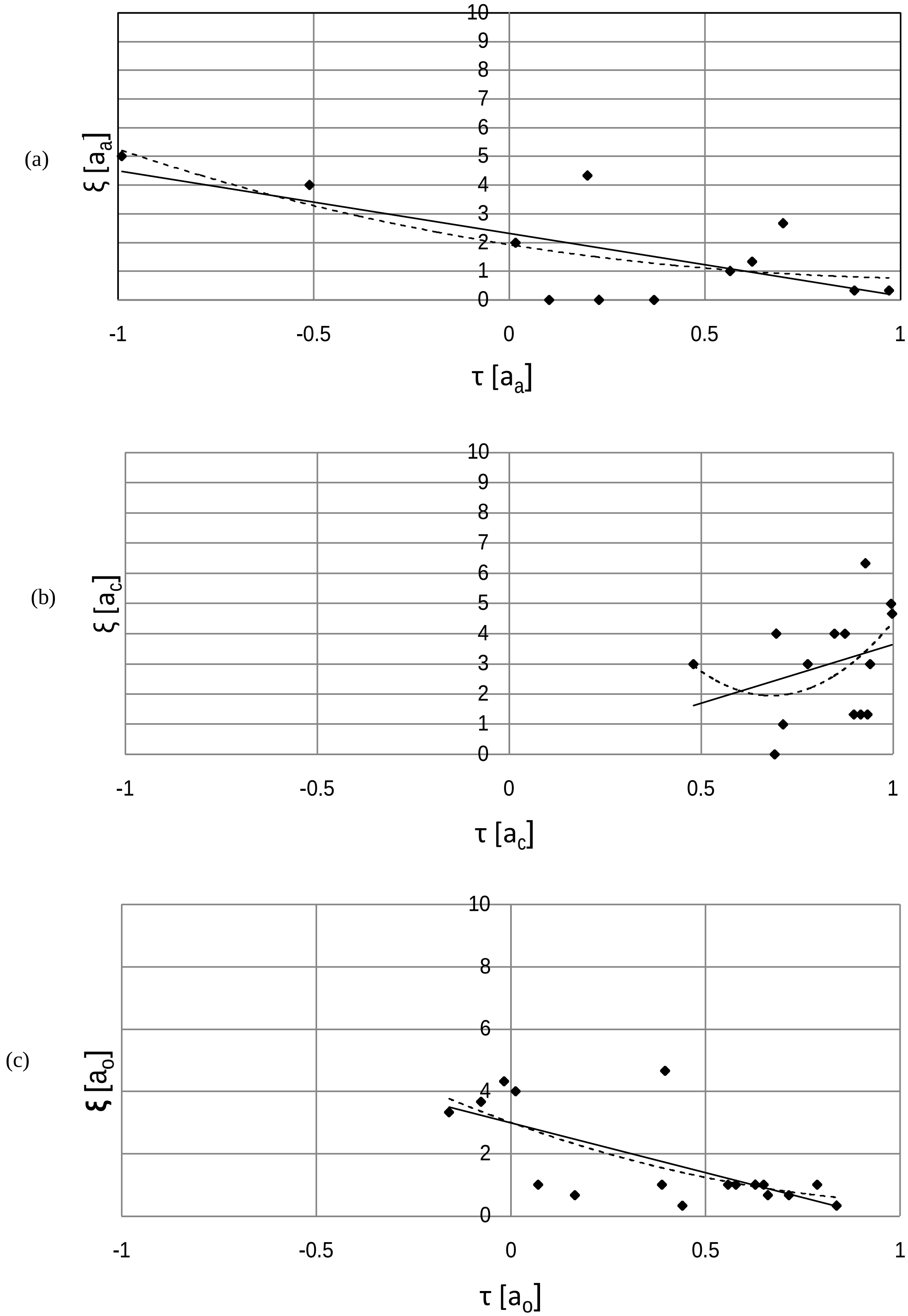

Figure-2

Scatter Diagram between τ and ξ for three different categories of slopes – (a) Anaclinal Slope Units, (b) Cataclinal Slope Units and (c) Orthoclinal Slope Units

Conclusion

Alignment of rock strata and their style of exposure on the surface of the hill slopes have a significant impact in determining the issues of stability of a particular geomorphic slope unit. This basic relationship is worthy to be examined vividly during the framing of land use plans over the slopes. Presently, the Himalayan Mountain slopes are being modified rapidly due to the augmented quest of developing tourism economy in the hilly tracts. The large scale infrastructural development plans and other heavy construction works may lead to further instability to hill slopes if the locations of such activities are not allocated rationally. Present study is the effort of establishing only one factor responsible for the slope instability in a particular river basin of Garhwal Himalaya; and the findings of the study unfold the scope of the verification and further extension of the particular issue; and, obviously, the inclusion of other factors may explain the situation more effectively. The rational decision making process in terms of hill slope land use and sustainable hill slope modification may be the answer of the dilemma of maintaining a rational balance between the development and the environmental conservation.

References

1. Smith K., Environmental Hazards: Assessing Risk and Reducing Disaster, Routledge, **2**, 4-11 **(1996)**
2. Fookes P. G. and Wilson D. D., The Geometry of Discontinuities and Slope Failures in Siwalik Clay, *Geotechnique*, **16**, **4**, 305–320 **(1966)**
3. Zaruba Q. and Mencl V., *Landslides and their control*, Academia Prague: Elsevier, 205 **(1969)**
4. Varnes D.J., Slope movement, types and processes, *Landslides analysis and control*, Washington, D.C.: National Academy of Sciences, **Special Report 176**, 11–33 **(1978)**
5. Esu F., Behaviour of slopes in structurally complex formations, *Capri*, **2**, 292–304 **(1977)**
6. Vv. Aa., *Geotechnical Engineering in Italy - An overview*, Published on the occasion of the ISSMFE Golden Jubilee, Roma, A. G. I.- Associazione Geotecnica Italiana, 414 **(1985)**
7. Guzzetti F., Cardinali M. and Reichenbach P., The influence of structural setting and lithology on landslide type and pattern, *Environ. Eng. Geosci.*, **2,4**, 531–555 **(1996)**
8. Scheidegger A.E., Tectonic predesign of mass movements: with examples from the Chinese Himalaya, *Geomorphology*, **26**, 37–46 **(1998)**
9. Cruden D.M. and Varnes D.J., Landslide Types and Processes, *Landslides: Investigation and Mitigation*, Washington D.C.: National Academy Press, 36–72 **(1996)**
10. Freeze R.A. and Cherry J.A., *Groundwater*, Englewood Cliffs: Prentice-Hall, 604 **(1979)**
11. Selby M.J., *Hillslope Materials and Processes*, Oxford: Oxford University Press, 451 **(1993)**
12. Indian Standard (IS): 1893-Part I, *Criteria for earthquake resistant design of structures*, New Delhi: Bureau of Indian Standard, **(2002)**
13. *Slope Instability Issues in the Areas around Mussorrie*, Dehradun: Disaster Mitigation and Management Centre, Govt. of Uttarakhand, **(2013)**
14. Meentemeyer R.K. and Moody A., Automated mapping of alignment between topography and geologic bedding planes, *Computers & Geosciences*, **26(7)**, 815-829 **(2000)**
15. Dozier J., A clear-sky spectral solar radiation model for snow-covered mountainous terrain, *Water Resources Research*,**16**, 709-718 **(1990)**
16. Dubayah R.C., Estimating net solar radiation using Landsat Thematic Mapper and digital elevation data, *Water Resources Research*, **28**, **(1992)**